

## STUDY OF NI-V LOAD ACID-MODIFIED CALCINED KAOLIN

LkhagvajavN<sup>1\*</sup>, Zhang Q<sup>2</sup>, Tsedendorj Ts<sup>3</sup>

1-Plant Protection Research Institute, MULS, Mongolia

2-Chemical engineering college, Inner Mongolia University of Technology, China

3-Institute of Chemistry and Chemical Technology, MAS, Mongolia

\*-Corresponding author, E-mail: [Nymsuren\\_lkhagvaa@yahoo.com](mailto:Nymsuren_lkhagvaa@yahoo.com)

### ABSTRACT

*Kaolin as a natural clay mineral, is commercially available at low costs, which is of great importance. It has been demonstrated by existing research kaolin is a very effective carrier for photocatalyst, being able to promote the photocatalytic reaction process as well as improve the efficiency of reaction. The catalysts was characterized by FT-IR, XRD, UV-Vis spectra methods. Ni and V, amount of catalyst investigate. Simultaneously the effects of photocatalytic reaction activity about concentration of sulfuric acid, calcination temperature, ratio of Ni and V, amount of catalyst investigate. The experimental results show that the photocatalytic activity of calcined kaolin which is treated by 40% and loading Ni and V is significantly higher than other kaolin. The kaolin does not have the B acid and L acid peaks, but people could see the B acid and L acid peaks on the kaolin which is roasted and treated by sulfuric acid. In a certain range, the activity of the catalysts in crease with the increasing of the concentration of acid.*

**KEYWORDS:** Kaolin, sulfuric acid, photocatalyst

### INTRODUCTION

TaoYL et al<sup>[1-2]</sup>. has done a lot of research, that the conversion rate of 1.4 pentanedione cobalt catalysts, substrates and illumination time is proportional to acetone as photosensitizer, the best can reach 100%. In recent 10 years, due to its semiconductor catalyst capable of initiating a redox reaction of the photocatalytic reactivity much attention<sup>[3]</sup>. The ultraviolet and visible light have also been shown to break the thermodynamic limit or promote effective means of thermodynamics is not suitable for the reaction<sup>[4]</sup>. Based on these, Wang et al<sup>[5]</sup>. The one-doped (Ni, V, O) semiconductor compound as the

catalyst, a fixed bed continuous flow reactor the catalyst, in order to enhance the activation of carbon dioxide, carbon dioxide, direct synthesis of methanol and catalytic dimethyl, dimethyl carbonat eyield increase, while continuously flowing fixed-bed reactor in time to take away the water produced by the reaction, the catalyst nano particle 4-8 nm to form an hydrous reaction system is conducive to dimethyl carbonate generate results show, with good light absorption characteristics.

## METHODS

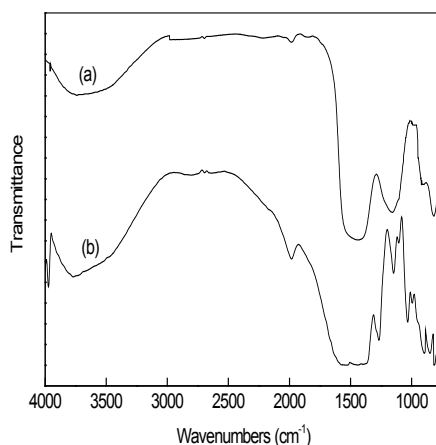
Added 200 mL of deionized water and a certain amount of ammonium vanadate in the flask, stirred and heated to 60°C until completely dissolved. Press different  $n(\text{Ni}^{2+}):n(\text{V}^{5+})$  added nickel nitrate and nickel nitrate configure a mixed solution of ammonium. After cooling by solid - liquid ratio of 1:5(g/mL) was added  $\text{SO}_4^{2-}/\text{CK}$ , heated to 90°C,

stirred at reflux for 2 h, allowed to stand for more than 20 hours, filtered, and the filter cake 110°C dried, milled calcined at different temperatures for 2 hours, acidified calcined kaolin supported Ni-V catalyst sample, referred to as Ni-V/  $\text{Y}\%\text{SO}_4^{2-}/\text{CK-X}$ , X is the sample firing temperature (°C).

## RESULTS AND DISCUSSION

Figure 1 is calcined at 500°C soil by 40%  $\text{H}_2\text{SO}_4$ -modified 40% $\text{SO}_4^{2-}/\text{CK}$  FTIR spectrum. According to the results of Figure.1 combined with references to analyze the spectral characteristics of the sample<sup>[6-9]</sup>. 500  $\text{cm}^{-1}$  and an absorption peak 900 ~ 1000 $\text{cm}^{-1}$  indicates  $\text{SO}_4^{2-}$  coordination between adsorption, which is the formation of acid sample center important conditions<sup>[13]</sup>. The Ni-V/40% $\text{SO}_4^{2-}/\text{CK-500}$  spectrum, the intensity of these peaks increased significantly, indicating the presence of Ni-V promotes coordination  $\text{SO}_4^{2-}$ - adsorption. In addition, Ni-V/40% $\text{SO}_4^{2-}/\text{CK-500}$   $\text{Ni}^{2+}$  and  $\text{SO}_4^{2-}$  is chemically bonded to the absorption peak of 440  $\text{cm}^{-1}$  is due to vibration Ni-S, instructions; absorption peak attributable to 600~700 $\text{cm}^{-1}$  between in V-O-V symmetric stretching vibration, the absorption peak of 700~800  $\text{cm}^{-1}$  between the anti symmetric

stretching vibration attributable to the V-O-V, the absorption peak of 1220  $\text{cm}^{-1}$  in the sample is caused by surface adsorption of  $\text{SO}_4^{2-}$ -V-O bond stretching vibration, indicating different  $\text{V}^{5+}$  and  $\text{Ni}^{2+}$  binding mode and the carrier. And 40% $\text{SO}_4^{2-}/\text{CK}$  in 1047 stretching vibration characteristic Si-O-Si  $\text{cm}^{-1}$  absorption peak compared, Ni-V of this absorption / 40%  $\text{SO}_4^{2-}/\text{CK-500}$  shifts to high wave number region and split, indicating a class isomorphous replacement presence.  $\text{Al}^{3+}$ ,  $\text{V}^{5+}$  and  $\text{Ni}^{2+}$  ionic radii 0.0535, 0.054 and 0.069 nm,  $\text{Al}^{3+}$  and  $\text{V}^{5+}$  relative error ionic radius of only 0.9%, while the  $\text{Ni}^{2+}$  and  $\text{V}^{5+}$  ion radius relative error of 22%, greater than 15%, so only  $\text{V}^{5+}$  There are baked earth with kaolinite Al-O octahedron activation occurs  $\text{Al}^{3+}$  class isomorphous replacement may<sup>[9]</sup>.



(a) 40% $\text{SO}_4^{2-}/\text{CK}$  (b) Ni/V/40% $\text{SO}_4^{2-}/\text{CK}$

Figure 1. FTIR spectra of samples

Figure 2  $\text{V}^{5+}$  and  $\text{Al}^{3+}$  class isomorphism replacement Fig.  $\text{V}^{5+}$  and Al-O octahedra occur in the  $\text{Al}^{3+}$  class isomorphous replacement, in order to compensate for  $\text{V}^{5+}$   $\text{Al}^{3+}$  substitution after excess positive charge, positive charge excess negative charge is captured to make to achieve balance within the crystal

electrically neutral. For the photocatalytic process, this process may capture photo-generated electrons, which would reduce the light-generated electron and hole recombination of photo-generated odds in favor of the photocatalytic activity of the catalyst.

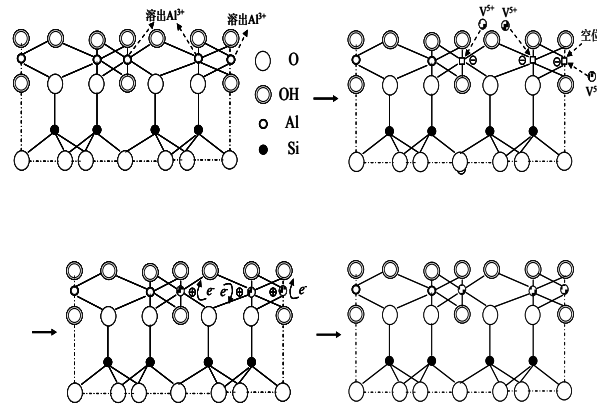
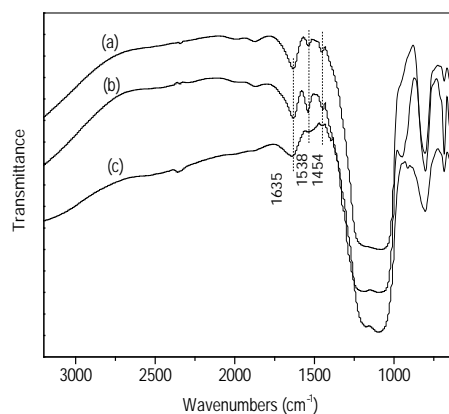


Figure 2. Schematic of isomorphism substitution process between  $V^{5+}$  and  $Al^{3+}$

Figure 3 is  $n(Ni^{2+}):n(V^{5+})=2:8$  impregnating solution prepared Ni-V/40%SO<sub>4</sub><sup>2-</sup>/CK-400<sup>0</sup>C, 500<sup>0</sup>C and 600<sup>0</sup>C of pyridine adsorption IR spectrum. As indicated by the sample in 1450,1540 and 1630 cm<sup>-1</sup> at a location nearby (1454,1538 and 1635 cm<sup>-1</sup>) absorption peaks appeared. Generally believed, 1540 cm<sup>-1</sup> appears at the Bronsted acid (B acid) bits and pyridine molecule pyridine and generated ions characteristic absorption peak, and the absorption peak at 1450 cm<sup>-1</sup> for the Lewis acid (L acid) position and pyridine molecule and generated complexes characteristic absorption at 1630 cm<sup>-1</sup> acid B and L acid superposition peak<sup>[10,11]</sup>. As can be seen from the figure, Ni-V/40%SO<sub>4</sub><sup>2-</sup>/CKs samples were simultaneously the B and L acid sites. Since H<sub>2</sub>SO<sub>4</sub> dissolution of kaolinite skeleton CK activated Al, part of the dissolution of Al present in the CK, the outer surface of the non-framework aluminum, has become a growth point of L acid sites<sup>[12]</sup>. In addition, in front of the FTIR results showed that CKSO<sub>4</sub><sup>2-</sup> adsorbed surface ligand, while the presence

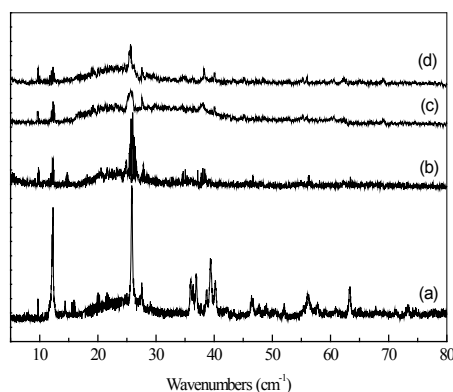
of Ni-V promotes coordination adsorption SO<sub>4</sub><sup>2-</sup>, SO<sub>4</sub><sup>2-</sup> induced effects in the S=O enhances the ability to seize electronic surface of the metal ions, strengthen the L acid sites; at the same time, the induced effect makes it easier to dissociate H<sub>2</sub>O adsorption to produce B acid sites<sup>[13]</sup>. B-hydroxy acid sites capture the light-activated Ni-V/40%SO<sub>4</sub><sup>2-</sup>/photogenerated holes after CKs surface can produce more hydroxyl radical ( $\bullet OH$ ); and L acid center electron-deficient, the photo-generated electrons flow L acid sites, reducing the light electrons and light green hole recombination probability. Meanwhile, the lack of electronic structure L acid is also conducive CH<sub>3</sub>OH adsorption and activation<sup>[14]</sup>, which help promote the activity of the catalyst. The figure can be seen, Ni-V/40% SO<sub>4</sub><sup>2-</sup>/CK-500 on B acid and L acid sites characteristic absorption peak intensity was significantly higher than the other two samples, indicating its total acid content of the largest in the three samples.



- (a) Ni-V/40%SO<sub>4</sub><sup>2-</sup>/CK-400
- (b) Ni/V/40%SO<sub>4</sub><sup>2-</sup>/CK-500
- (c) Ni-V/40%SO<sub>4</sub><sup>2-</sup>/CK-600

Figure 3. Py-FTIR spectra of samples obtained at different calcination temperatures

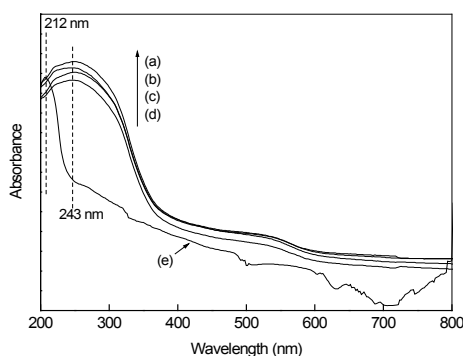
Figure 4 is the original soil K, 500°C calcinat CK, weakened further described by H<sub>2</sub>SO<sub>4</sub> after CK 40%SO<sub>4</sub><sup>2-</sup>/CK and Ni-V/40% SO<sub>4</sub><sup>2-</sup>/CK-500 XRD patterns. Ni-V/40%SO<sub>4</sub><sup>2-</sup>/CK-500 is n(Ni<sup>2+</sup>):n(V<sup>5+</sup>)=2:8 prepared impregnating solution. CK figurethe spectrum, kaolinite characteristic peak intensity was significantly reduced, the two three-finger peak between 35° and 40° has been destroyed, indicating that the original soil after calcinations at 500°C, kaolinite oxyeight icosahedral structure was damaged, the structure was activated aluminum; each characteristic peak intensity 40%SO<sub>4</sub><sup>2-</sup>/CK kaolinite



(a) original kaolin (b)CK (c)40%SO<sub>4</sub><sup>2-</sup>/CK(d)Ni-V/40%SO<sub>4</sub><sup>2-</sup>/CK-500  
Figure 4. XRD patterns of different samples

Figure 5 is 40%SO<sub>4</sub><sup>2-</sup>/CK and n(Ni<sup>2+</sup>):n(V<sup>5+</sup>)=2:8, 4:6, 6:4 and 8:2 impregnating solution prepared supported catalyst Ni-V/40% SO<sub>4</sub><sup>2-</sup>/UV-Vis CKs-500 test results. The figure can be seen, with 40%SO<sub>4</sub><sup>2-</sup>/CK compared, Ni-V maximum absorption / 40%SO<sub>4</sub><sup>2-</sup>/CKs-500 appears red-shifted by 212 nm red shift near 243 nm. As mentioned above, V<sup>5+</sup> class isomorphous substitution Al<sup>3+</sup> appear after excess positive charge, in order to achieve the crystal charge balance, the negative charge will flow positive charge excess, the electron density decreases leading to red shift of the maximum absorption peak<sup>[15]</sup>. Meanwhile, the absorbance intensity Ni-V/40%SO<sub>4</sub><sup>2-</sup>/CKs-500 samples

representing 40%SO<sub>4</sub><sup>2-</sup>/CK are greatly improved, indicating synergy Ni-V will increase the light absorption properties of the sample. Which are conducive to the promotion of the photocatalytic activity of the catalyst. N(Ni<sup>2+</sup>):n(V<sup>5+</sup>)=2:8 maximum absorbance of the sample. In addition, different n(Ni<sup>2+</sup>):n(V<sup>5+</sup>) prepared Ni-V/40% SO<sub>4</sub><sup>2-</sup>/CK-500 absorption sidebands are obvious red shift. Sideband absorption redshift means reduced bandgap. The band gap is smaller, the wide range of optical response of the sample, and can absorb more photons<sup>[16]</sup>. The results show that UV-Vis spectra of doped beneficial light absorption properties, the promotion of photocatalytic activity of the sample.



(a) 2:8 (b) 6:4 (c) 8:2 (d) 4:6 (e) 40%SO<sub>4</sub><sup>2-</sup>/CK  
Figure 5. UV-Vis patterns of samples with varied (Ni<sup>2+</sup>):n(V<sup>5+</sup>)

## CONCLUSIONS

Calcined kaolin important factor in the emergence of surface-modified (L) H<sub>2</sub>SO<sub>4</sub> acid (B) acid center, with H<sub>2</sub>SO<sub>4</sub>-modified calcined kaolinas carrier Ni-V-supported photocatalyst, the surface acidity is to promotethe photocatalytic activity.

Ni-V occurred V<sup>5+</sup> and Al<sup>3+</sup> class isomorphous substitution and changed the electronic distribution

of the catalyst surface, suppressing the optical excitation composite surface of photo-generated electrons and photogenerated holes and improves the catalysts H<sub>2</sub>SO<sub>4</sub>-modified calcined kaolin load the response performance.

## REFERENCE

1. Tao Y L, Yeh W L, Chow Y L. Acidity effects on Light-promoted carbonylation of olefins in the presence of cobalt catalysis [J] *J MolCatal*, 1991, 67(1): 105-115.
2. Tao Y L, Tashin J, Chow J T, Lin Ch Ch, Chien M T, Lin Ch Ch, Chow Y L, Gonzalo E. Cobalt-catalysed photochemical methoxy carbonylation of olefins under ambient conditions [J]. *J Chem Soc Perkin Trans*, 1989, 12: 2509-2511.
3. Linsebigler A L, Lu G G, Yates J J T. Photocatalysis on TiO<sub>2</sub> Surface: Principles, Mechanism, and Selected Results [J]. *Chem Rev*, 1995, 95(3): 735-758.
4. Emeline A V, Otroschenko V A, Ryabchuk V K, et al. A biogenesis and photosimulated heterogeneous reactions in interstellar media and on primitive Earth, Relevance to the Genesis Life [J]. *J Photochem Photobiol C: Photochem Rev*, 2003, 3(3): 203-224.
5. Wang X J, Xiao M, Wang S J, et al. Direct synthesis of dimethyl carbonate from carbon dioxide and methanol using supported copper (Ni, V, O) catalyst with photo-assistance [J]. *J Mol Catal A: Chem*, 2007, 278 (1-2): 92-96.
6. A. L. Linsebigler, G. Lu, J. T. Yates. Photocatalysis on TiO<sub>2</sub> Surface: Principles, Mechanisms, and Selected Results [J]. *Chemical Review*, 1995, 95(3): 735-758
7. Xu Rui, Tong Shi Tang photocatalytic activity of titanium dioxide and its modification [J] *Wuhan University of Science and Technology (Natural Science)*, 2001, 24(4): 358-360
8. Yu Jianguo, Zhao build heterogeneous photocatalysis on semiconductors principle and its application in environmental protection in the [J] *Wuhan University of Technology*, 2000, 22(4): 12-15
9. Shen Wei Ren, Zhaowide, HE Fei TiO<sub>2</sub> photocatalytic reaction and its application in wastewater treatment [J]. *Progress in Chemistry*, 1998, 10 (4): 349-361
10. Yang Jian jun, Li Dongxu, Zhang Zhi jun Pt preparation, characterization and photocatalytic activity of Fe<sub>2</sub>O<sub>3</sub> / TiO<sub>2</sub> [J]. *Vacuum Science and Technology*, 2001, 21 (4): 277-280
11. Jane Li, Zhang future cobalt Preparation and photocatalytic properties of titanium dioxide [J]. *Doping Environmental Science and Technology*, 2003, 26: 6-7
12. X. Z. Ding, X. H. Liu, Y. Z. He. Structural Evolution of Gel-Derived Nano crystalline Titania Powders Doped with Ferric Oxide [J]. *J. Mater. Sci. Letters*, 1996, 15(16): 1392-139
13. Shouew, Liu Hong photocatalysis and Photoelectrocatalytic Fundamentals and Applications [M] Beijing: Chemical Industry Press, 2005
14. A. E. S. LEE, et al. Methyl formate Preparation [J]. *Applied Catalysis*. 1990, 57: 1-30
15. M. Gratzel, F. H. Ruessell. Electron Paramagnetic Resonance Studies of doped TiO<sub>2</sub> Colloids [J]. *J. Phys. Chem*, 1990, 94(6): 2566-2572
16. Fei Sun Yi, the activity of wastewater [J] Li Xiao bo TiO<sub>2</sub>/ACFs Photocatalytic Degradation of Environmental Science and Technology, 2012, 35(5): 102: 105